Published in final edited form as:
J Invest Dermatol. 2009 June ; 129(6): 1367–1378. doi:10.1038/jid.2008.380.

Vitamin D Receptor and Coactivators SRC2 and 3 Regulate Epidermis-Specific Sphingolipid Production and Permeability Barrier Formation

Yuko Oda[1], **Yoshikazu Uchida**[2], **Sam Moradian**[2], **Debra Crumrine**[2], **Peter M. Elias**[2], and **Daniel D. Bikle**[1,2]

[1] Department of Medicine, University of California, San Francisco, California, USA

[2] Department of Dermatology, University of California, San Francisco and Veterans Affairs Medical Center San Francisco, San Francisco, California, USA

Abstract

The vitamin D receptor (VDR) is a nuclear hormone receptor that controls transcription of target genes. It exerts its biological effects through transcriptional coactivators. Previously, we identified two distinct classes of VDR coactivators, VDR-interacting protein (DRIP) and steroid receptor coactivator (SRC) at different stages of keratinocyte differentiation. Here, we determined the functions of VDR and coactivators in lipid production and permeability barrier formation. Silencing of either VDR, SRC2, or SRC3 resulted in decreases in specific glucosylceramide (GlcCer) species but not other lipids such as cholesterol and free fatty acids. Their silencing also caused decreased transcription of fatty acid elongase and ceramide glucosyltransferase, which are critical for the synthesis of epidermis-unique GlcCer species, and defects in lamellar body formation associated with decreased expression of the lipid transporter ATP-binding cassette transporter protein 12. VDR null mice exhibit abnormal barrier function with altered lipid composition *in vivo*. These results demonstrate that VDR and coactivators SRC2 and SRC3, which are also involved in other nuclear receptors as well, are critical for epidermis-specific sphingolipid production and barrier formation. In contrast, DRIP silencing had no apparent effect on these processes indicating that the two classes of coactivators are differentially utilized.

INTRODUCTION

The vitamin D receptor (VDR) is a nuclear hormone receptor that controls transcription of target genes and regulates proliferation and differentiation of various cells including epidermal keratinocytes (Haussler *et al*., 1998). Binding of 1,25 dihydroxyvitamin D3 to VDR stimulates its transcriptional activity. In cultured human epidermal keratinocytes, VDR by 1,25-dihydroxyvitamin D3 induces differentiation through increased transcription of early differentiation markers involucrin and transglutaminase (reviewed by Bikle, 2004). We previously identified a DR3-type VDR response element sequence adjacent to a critical AP-1 site in the involucrin promoter (Ng *et al*., 2000). However, the direct function of VDR in two important aspects of epidermal keratinocytes, namely lipid production and epidermal barrier formation, has not been previously evaluated.

Correspondence: Dr Yuko Oda, Endocrine Research (111N), Veterans Affairs Medical Center San Francisco, 4150 Clement Street, San Francisco, California 94121, USA. yuko.oda@ucsf.edu.

CONFLICT OF INTEREST

The authors state no conflict of interest.

One of the most important functions of epidermal keratinocytes is to generate a permeability barrier, which prevents both pathogen invasion and excess transcutaneous water loss in the skin (Elias, 2007) essential for the survival of terrestrial mammals. The epidermal permeability barrier resides in the outermost epidermal layer, the stratum corneum (SC; Elias, 2005). The lipids involved in the formation of the barrier are synthesized in the stratum granulosum (SG), and are assembled as their precursors within organelles, the epidermal lamellar bodies (LBs; Schurer and Elias, 1991). LB contents are then secreted between the SG and the SC, and hydrolytically processed within the extracellular spaces, eventually forming the lamellar bilayers that mediate permeability barrier function (Holleran *et al*., 2006). The mammalian SC contains large quantities of lipids, which are primarily comprised of equal mixtures of ceramides (Cer), cholesterol, and free fatty acid (FA; Elias and Menon, 1991). Because of their large molecular mass, Cer consist approximately half of the total lipid content by weight. These Cer are represented by at least 10 species (designated Cer 1–10) due to variations in sphingol (or sphingoid base) structures, and/or non-hydroxy, α (or 2)- or ω-hydroxylation of the amide-linked FA (Uchida and Holleran, 2008; Table 1). These Cer are characterized by differences in N-acyl FA structures, including 2-hydroxylation, desaturation, and unusually long carbon chain length (>C30). Not only bulk amounts of Cer, but also the molecular heterogeneity of these Cer is critical to form a competent epidermal permeability barrier. In particular, Cer 1 (also called EOS), Cer 4 (EOH), and Cer 9 (EOP), are unique to the epidermis. These Cer species contain very long chain amide-linked AF with terminal ω-hydroxy groups and are further esterified. Their syntheses are increased at the late stage of epidermal differentiation (Holleran *et al*., 2006; Uchida and Holleran, 2008).

Some of the enzymes that catalyze Cer/GlcCer production have been characterized (Holleran *et al*., 2006; Figure 6). Serine palmitoyl transferases (SPT) 1 and SPT2 mediate the first step in all Cer/GlcCer syntheses. Desaturases 1 and 2 (DES1, DES2) account for sphingol (or sphingoid base) synthesis (Holleran *et al*., 2006). FA elongases ELOVL3 and 4 are required for the synthesis of epidermis-specific very long chain FA (Uchida and Holleran, 2008). Fatty acid 2-hydroxylase (FA2H) accounts for the synthesis of α (or 2)-hydroxylated FA formation (Uchida *et al*., 2007). All Cer species are converted to precursors and stored in LB as glucosylceramide (GlcCer) or sphingomyelin (SM), which are synthesized by ceramide glucosyltransferase (UGCG) and SM synthase, respectively (Holleran *et al*., 2006). Acid sphingomyelinase (SMPD1) and/or neutral sphingomyelinase (SMPD2), which convert SM to Cer, have an important function in barrier formation (Jensen *et al*., 1999, 2004, 2005). Another processing enzyme, β-glucocerebrosidease (GBA) generates Cer from GlcCer.

Finally, the ATP-binding cassette transporter protein 12 (ABCA12) appears to be important as a lipid transporter to facilitate the assembly of these precursors within epidermal LB. Our previous studies and those of others showed that disrupted function of ELOVL3 (Westerberg *et al*., 2004; Jakobsson *et al*., 2006), ELOVL4 (Vasireddy *et al*., 2007), FA2H (Uchida *et al*., 2007), UGCG (Jennemann *et al*., 2007), or ABCA12 (Akiyama *et al*., 2005) results in abnormal barrier function, indicating their critical role in permeability barrier homeostasis.

Inherited alterations of Cer or GlcCer metabolism also promote skin diseases that display barrier abnormalities, such as Gaucher's disease (Holleran *et al*., 1994; Sidransky *et al*., 1996), Harlequin ichthyosis (Akiyama *et al*., 2005). Recently, it was reported that mutations in ABCA12 cause Harlequin ichthyosis (Akiyama *et al*., 2005; Thomas *et al*., 2006), in which abnormal LBs are observed. Here we asked whether VDR and its coactivators regulate the synthesis of one or more of these lipids, and the degree to which this regulation impacts permeability barrier homeostasis.

VDR exerts its biological effects through ''coactivators''. A number of coactivators have been recently described that are essential for the function of nuclear hormone receptors like VDR

to activate transcription. These coactivators are postulated to be critical for the tissue- or stage-specific action of nuclear receptors. Using GST–VDR affinity beads and mass spectrometry, we previously purified and identified two VDR coactivator complexes from keratinocytes at different stages of differentiation, and found that they have different functions during keratinocyte differentiation (Oda *et al*., 2003, 2007). One complex is the VDR-interacting protein (DRIP) complex, which is involved in VDR transactivation in undifferentiated proliferating keratinocytes (Oda *et al*., 2003). The DRIP complex (Blazek *et al*., 2005; Kornberg, 2005), also known as ‘‘Mediator’’ (Bourbon *et al*., 2004) also mediates the function of other nuclear hormone receptors and transcription factors such as the TR, PPAR, and BRCA1 (Blazek *et al*., 2005). A second class of coactivators is the steroid receptor coactivator (SRC) family, also known as p160 coactivators (reviewed in Leo and Chen, 2000). Two members of this family, SRC2 (also called TIF2/GRIP1/NcoA-2) and SRC3 (also called RAC3/pCIP/ACTR/AIB1/TRAM-1), were identified in differentiated keratinocytes (Oda *et al*., 2003). SRC3 mediates VDR activity in differentiated keratinocytes (Oda *et al*., 2003). These previous results suggest a model in which DRIP is the dominant coactivator complex in proliferating keratinocytes, but is replaced by SRC family members as the keratinocytes differentiate (Oda *et al*., 2003). Here we further test this model in fully differentiated keratinocytes, where epidermis-specific sphingolipids are produced like those that form the permeability barrier in the epidermis. Specifically, epidermal lipid production and barrier formation can be induced in a vitamin C and serum-supplemented submerged culture system (Uchida *et al*., 2001), where keratinocytes form barrier layers resembling those of the *in vivo* epidermis.

We examined the function of VDR and coactivators by blocking their expression in cultured human epidermal keratinocytes, using short-interferance (siRNA) silencing technology. To confirm these *in vitro* results we then examined the epidermis of VDR null mice (Yoshizawa *et al*., 1997) with respect to LB secretion, barrier function, and lipid composition.

RESULTS

VDR and coactivators SRC2 and SRC3 regulate epidermis-specific glucosylceramide production

To examine the function of VDR and coactivators in lipid production and barrier formation, the expression of each was blocked using siRNA-silencing technology. Among multiple DRIP subunits, DRIP205/Med1 was targeted because it directly binds to VDR through its NR boxes and is critical in transcriptional activation (Oda *et al*., 2003). Two SRC family members, SRC2 and SRC3, were also targeted because they were identified in differentiated keratinocytes (Oda *et al*., 2003). Human epidermal keratinocytes were infected with adenovirus encoding short-hairpin RNA (shRNA) for VDR, DRIP205, SRC2, and SRC3 (75 IFU per cell) to block their expression. These cells were then compared to controls infected with control adenovirus. The blocking efficiency for VDR and the coactivators was previously measured: VDR 55%, DRIP 65%, SRC2 53%, SRC3 40% for mRNA, and VDR 70%, DRIP 90%, SRC2 60%, SRC3 80% for protein (Hawker *et al*., 2007). Epidermis-specific lipid production and barrier formation were stimulated in a vitamin C and serum-supplemented submerged culture system (Uchida *et al*., 2001), in which keratinocytes form barrier layers resembling those of epidermis *in vivo*. The infected keratinocytes were maintained in vitamin C-supplemented serum for an additional 5–10 days to allow formation of a multilayered, epidermis-like tissue, where barrier lipids are synthesized and barrier-like structures become evident. We first assessed the relative levels of the immediate precursors of barrier Cer; that is, GlcCer and SM (Figure 1a). When VDR was silenced, total GlcCer (open bars) but not SM levels decreased (Figure 1a, left graph). Silencing SRC2 and SRC3, but not DRIP, also significantly decreased total GlcCer (Figure 1a, right graph open bars). As epidermal GlcCer comprise a heterogeneous family, which leads

to the heterogeneity of Cer species in the SC (Table 1), we next investigated the distribution of individual GlcCer fractions. When VDR was silenced, all GlcCer decreased, with a decline in epidermis-specific acylCer species being most significant (Figure 1a, left graph). When either SRC2 or 3 was silenced, all GlcCer decreased, with the decline in acylGlcCer and GlcCer D fractions being most substantial (Figure 1a, right graph). Consistent with the decrease in acylGlcCer in SRC2- and SRC3-silenced cells, there was also a substantial decline in Cer 1 (acylCer), the deglucosylated form of acylGlcCer (Figure 1b, right graph). In addition, Cer 6 +7 (Cer6/7), which are primarily derived from GlcCer C and D, also decreased when either SRC2 or SRC3 were silenced (Figure 1b, right graph). Although acylCer, Cer 6/7 and their precursors acylGlcCer and GlcCer B, C, D decreased in VDR-silenced cells (Figure 1a, left graph), the levels of Cer 2–5 were not significantly diminished (Figure 1b, left graph). In contrast, DRIP silencing did not significantly decrease either total GlcCer or Cer levels, although a significant increase in Cer 1 and Cer 2 (containing C16 as major amide-linked FA) and a moderate decline in the levels of GlcCer D and Cer 3–5 occurred (Figure 1a,b right graphs). Finally, we also assessed the other major barrier lipid species, cholesterol and FA. The levels of these lipids were not significantly diminished when either VDR or coactivators were blocked (Figure 1c). Together, these data demonstrate that VDR and coactivators SRC2 and SRC3, but not DRIP, regulate the production of GlcCer species, which are the immediate precursors of barrier-specific Cer.

VDR and coactivators SRC2 and 3 are critical for barrier formation

We next assessed whether the siRNA-induced decrease in sphingolipid production results in abnormalities in permeability barrier formation. We used high-resolution electron microscopy to examine cultured keratinocytes for their ability to carry out four key steps in barrier formation: (1) stratification, (2) LB formation, (3) lipid secretion, and (4) postsecretory lipid processing (Table 2). Stratification was assessed as the extent of formation of organelle depleted flattened corneocyte layers enclosed by a cornified envelope. LB formation was evaluated as the number, density (per μm^2 cytosol) of LBs and the lamellar contents of individual LBs in osmium tetroxide postfixed samples (Figure 2a, c, e and g). Finally, LB secretion and processing of secreted lipids into lamellar bilayers within the extracellular spaces were assessed by postfixation with ruthenium tetroxide (Hou *et al*., 1991;Figure 2b, d, f, and h). Control tissues infected with control adenovirus showed significant stratification and cornification, as well as a reasonable density of LBs, some of which secreted their contents into the extracellular spaces (Figure 2a, triangles). Most of these organelles exhibited internal lamellar contents (Figure 2b, shown by left triangle pointed to LB). In addition, organelle secretion and post-secretory processing into mature extracellular lamellar membrane structures were readily observed (Figure 2b, space shown between opposing two right triangles). These results indicate that control keratinocytes grown in vitamin C-supplemented media and serum generate normal LBs and downstream formation of lamellar bilayers (summarized in Table 2), as occurred in the epidermis *in vivo* as previously described (Uchida *et al*., 2001). In contrast, when VDR was silenced, both incomplete stratification and abnormal lamellar bilayer formation were observed (Figure 2c and d; Table 2). In these VDR-silenced tissues, we also found decreased numbers of LBs, and individual LBs often lacked typical lamellar contents (Figure 2c, triangles). In addition, very little LB secretion appeared to occur into the extracellular spaces in VDR-silenced cells (Figure 2d).

When SRC2 was silenced, similar, but unique abnormalities were observed. Although there was a relatively normal density of LBs in the cytosol of SRC2-silenced cells, many LB again lacked internal lamellar structures (Figure 2e, closed triangles), reflected by the secretion of empty vesicles into the extracellular spaces (Figure 2e, open triangles). Finally, mature lamellar bilayer structures were not evident, indicating abnormal postsecretory processing (Figure 2f). SRC3-silenced cells showed even further abnormalities, that is, no stratification, no LB

formation, and no lamellar bilayers (Figure 2g and h), indicating that silencing of this gene adversely affected the entire differentiation process (Table 2). In contrast, when DRIP205 was blocked, stratification was incomplete, but a reasonable number of LBs, replete with internal lamellar content and relatively normal appearing lamellar bilayers, were observed (Table 2). These results demonstrate that VDR and coactivators SRC2 and 3 are important in LB formation and secretion. SRC3 appears to block terminal differentiation at a step before barrier formation. In contrast, DRIP205 shows only a limited role in LB formation and secretion. These results are consistent with our previous observation that DRIP and SRC have differential functions in VDR regulation during keratinocyte differentiation, with DRIP being critical in undifferentiated keratinocytes, whereas SRC family members have the dominant role as keratinocytes differentiate.

VDR null mice have disrupted barrier formation, lipid secretion, and lipid composition

We next examined the *in vivo* role of VDR using a mouse model in which VDR is disrupted (Yoshizawa *et al*., 1997). Previously, we showed that VDR null mice develop alopecia with grossly distorted hair follicles, and subtle changes in interfollicular epidermal differentiation (Xie *et al*., 2002). Here, we analyzed the ultrastructure of the epidermis of these mice at 4 and 6 weeks of age to determine whether there were changes in LB formation, lipid secretion/processing, or basal barrier formation. Wild-type mice showed normal LB formation (Figure 3a, closed triangles) and lipid secretion (Figure 3a, open triangles), and normal barrier formation shown by exclusion of lanthanum tracer from the SC (Figure 3c). In contrast, VDR null mice (6 weeks old) contained a decreased number of LBs and a reduced density of LB contents in the SG (Figure 3b, closed triangles). Abnormal lipid secretion was indicated by the disorganized structures both at the SG–SC interface (Figure 3b, closed triangles) and at the lower layers between cells of the SG where lipid secretion does not normally occur (Figure 3b, open triangles). Abnormal barrier formation also was observed by tracer experiment (Figure 3d). In contrast, lipid processing was relatively normal in VDR null mice (data not shown). Similar defects, including fewer LBs and abnormal lipid secretion, were observed in 4-week-old VDR null mice (data not shown). The lipid composition of VDR null mice was also altered. Wild-type mice had approximately an equal proportion of the three major lipids, cholesterol, FA, and Cer (1:1:1), important for the formation of a competent barrier structure. VDR null mice showed distinctly unequal proportions of these lipids, in that both cholesterol and FA were significantly increased compared to Cer (Figure 3e). This imbalance could affect LB structures and cause defects in barrier function. Accelerated lipid production is commonly observed to compensate for barrier defects in mouse models. However, in the VDR null mouse, epidermis-specific species of Cer (acylCer 1+Cer 4) did not increase, but the major constituent of Cer (Cer 2) did increase (Table 3). The proportion of epidermis-specific species vs general species (acylCer 1+Cer4/Cer 2) decreased in VDR null mice (Figure 3f). The ratio of acylGlcCer, precursors of acylCer, compared to GlcCer B, major precursor of Cer 2, also decreased (Figure 3f). These results indicate altered Cer distribution, in particular, a decrease in acylCer/acylGlcCer as well as changes in three major lipid composition, which also could affect epidermal barrier formation in VDR null mice.

Together, these data provide both a structural and a chemical bases for the permeability barrier abnormality in VDR null mice, and demonstrate that VDR is critical for lipid production, LB formation, lipid secretion, and barrier formation, in mouse skin.

VDR, SRC2, and SRC3 regulate very long FA elongases ELOVL3 and 4, UGCG, and lipid transporter ABCA12

Next, we explored the mechanisms by which VDR and coactivator SRCs regulate GlcCer synthesis and barrier formation in cultured human keratinocytes. The transcription of the genes for several key enzymes involved in these processes was evaluated by measuring changes in

mRNA levels using quantitative real-time PCR (Figure 4). Because VDR and coactivators SRC2 and 3 regulate Cer/GlcCer synthesis, we focused on the enzymes that synthesize these lipids (Figure 6). First, the mRNA expression of SPT1 and SPT2, which mediate the first step in sphingol synthesis, was assessed. The transcription of SPT1 and SPT2 was not affected when either VDR or coactivators was blocked. Expression of the desaturase enzymes, DES1 and DES2, decreased on VDR silencing, but their expression was not affected by the silencing of the coactivators, suggesting that other coactivators may be involved, or that the role of VDR in their expression is indirect. FA2H, which is required for α (or 2-) hydroxylation of FA to generate Cer 5 (AS), Cer 6 (AP), and Cer 7 (AH), was not affected by depletion of VDR and coactivators. In contrast, the mRNA level of ELOVL4, which was recently shown to be essential for N-acyl FA chain elongation, a key step in acylCer and acylGlcCer synthesis, was significantly decreased when either VDR, SRC2, or SRC3 was silenced (Figure 4). As anticipated, blockage of DRIP did not significantly affect ELOVL4 mRNA levels (Figure 4). Another member of the elongase superfamily, ELOVL3, was similarly affected by VDR silencing. However, the basal level of ELOVL3 was approximately 100-fold less than that of ELVOL4. The expression (Figure 4) and enzyme activity of UGCG (Figure 5) were also reduced by silencing VDR and coactivators DRIP, SRC2, and SRC3. DRIP silencing was less effective than that of SRCs with respect to UGCG expression and activity (Figures 4 and 5). UGCG catalyzes the conversion of *de novo* synthesized Cer into GlcCer, which is a prerequisite for loading into LBs. The enzymes responsible for lipid processing, GBA and acid and neutral sphingomyelinases (SMPD1, 2), were not regulated by VDR and coactivators (Figure 4).

Finally, we evaluated whether VDR regulates the expression of the lipid transporter, ABCA12, in part because similar abnormalities, that is decreased GlcCer and empty LB, occur in the inherited skin disorder Harlequin ichthyosis. When either VDR, SRC2, or SRC3 was blocked, ABCA12 expression significantly decreased, but DRIP silencing did not affect ABCA12 expression (Figure 4). Together, these results indicate that VDR and coactivators SRC2 and SRC3 regulate specific enzymes in the acylCer/GlcCer synthetic pathway, including steps involved in the elongation of FA (ELOVL), Cer glucosylation (UGCG), and lipid loading into LB (ABCA12) (Figure 6, shown by closed triangles).

DISCUSSION

We have demonstrated that VDR and coactivators SRC2 and SRC3 regulate the production of specific Cer and GlcCer species, which are increased at a late stage of keratinocyte differentiation in parallel to barrier formation. We have also investigated the potential mechanisms through which VDR and coactivators affect these processes. When either VDR, SRC2, or SRC3 was silenced, acylCer/acylGlcCer decreased, which may be explained by the decreased expression of elongase ELOVL4 responsible for the synthesis of unusually long-chain (C>30) FA included in epidermis-specific acylCer (Vasireddy *et al*., 2007). In addition, decreased ELOVL3 expression also accounts for decreases in the production of certain GlcCer (for example, C 22–26) (Westerberg *et al*., 2004). Furthermore, the decreased total GlcCer content may result from the decreased expression of UGCG, which mediates glucosylation of Cer. In contrast, FA2H (Uchida *et al*., 2007), SPT1, and SPT2, which are important for all Cer/GlcCer synthesis during differentiation, were also not regulated by VDR. Thus, our results indicate that VDR and coactivators SRC2 and 3 regulate specific steps in Cer/GlcCer synthesis, probably through ELOVL 3, 4, and UGCG (Figure 6).

When VDR, SRC2, or 3 expression was blocked, we observed incomplete barrier function with abnormal LB formation and lipid secretion, as well as decreased GlcCer levels. These findings may be explained by the decreased expression of ABCA12. Similar findings have been reported for the skin disease, Harlequin ichthyosis, which is associated with mutations in the *ABCA12*

gene, abnormal LB and lipid secretion, and decreased GlcCer production (Akiyama *et al*., 2005).

Previously we showed that mutant ELVOL4 knock-in mice show postnatal death because of severe barrier defects and lack of acylCer/GlcCer production (Vasireddy *et al*., 2007). Targeted disruption of ELOVL3 (Westerberg *et al*., 2004; Jakobsson *et al*., 2006) and UGCG (Jennemann *et al*., 2007) also results in abnormal permeability barrier function. Taken together with prior *in vivo* studies, our studies show a critical role for VDR and coactivators SRC2 and 3 in cutaneous barrier function probably through regulation of UGCG, ELOVL4, and ABCA12.

As VDR and coactivators regulate early, as well as late differentiation markers (Hawker *et al*., 2007), one might predict that silencing of VDR and coactivators would retard all stages of lipid synthesis, secretion, or processing. However, our results indicate that VDR and coactivators regulate specific GlcCer species and some of the enzymes such as ELOVL and UGCG involved in their synthesis during the later stages of differentiation.

VDR most likely utilizes SRC2 and 3 as its coactivators to regulate lipid production and barrier formation because similar defects were observed in these processes when either coactivator was silenced. However, silencing of SRC3 resulted in more severe morphological defects than did silencing of VDR or SRC2. Neither SRC2 nor 3 is specific for VDR, and their effects may be mediated by other transcription factors or nuclear receptors such as LXR and PPAR, which have also been found to impact keratinocyte differentiation.

DRIP silencing did not affect either lipid production or the expression of ELOVL4 and ABCA12. These data support our model in which the two coactivator complexes, DRIP and SRC, are differentially utilized during keratinocyte differentiation. We initially suggested a model in which DRIP is the dominant coactivator in proliferating keratinocytes, but is replaced by SRC family members as the cells differentiate (Oda *et al*., 2003). However, some of our observations do not entirely support our initial model. DRIP205 is localized in differentiated as well as proliferating keratinocytes (Schauber *et al*., 2008) and regulates the expression of the late differentiation markers loricrin and filaggrin (Hawker *et al*., 2007). On the other hand, we have demonstrated that in keratinocytes SRC2 and SRC3, but not DRIP, regulate cathelicidin, which mediates the innate immune response in the outermost layers in the skin (Schauber *et al*., 2008). We now modify our previous model by proposing that VDR utilizes DRIP to regulate cell proliferation, that VDR utilizes all three coactivators during the earlier and mid stages of differentiation, but that SRC2 and SRC3 are more critical for the terminal differentiation processes including barrier formation and innate immunity.

In summary, we have demonstrated that VDR and coactivators SRC2 and 3 are required for the production of epidermal-specific GlcCer and subsequent barrier formation. We linked these functions of VDR to regulation of the lipid transporter ABCA12 and ceramide synthetic enzymes ELOVL4 and UGCG. These functions of VDR, in turn, specifically required the SRC family of coactivators. DRIP involvement is limited, supporting our model of the differential utilization of the two coactivator classes by VDR during different stages of keratinocyte differentiation.

MATERIALS AND METHODS

Cell culture

Normal epidermal keratinocytes were isolated from neonatal human foreskin and grown in serum-free keratinocyte growth medium (CK) (Cascade Biologics, Portland, OR) with reduced EGF concentration as previously described (Gibson *et al*., 1996). Second, passage

keratinocytes were cultured with CK medium containing 0.03mM calcium for 3 days to allow for their proliferation. To induce terminal differentiation, maximum lipid synthesis, and barrier formation, cells were switched to medium containing DMEM and Ham F-12 (3:1, v/v), 50 $\mu g ml^{-1}$ vitamin C, 10% fetal bovine serum, 10 $\mu g ml^{-1}$ insulin, 0.4 $\mu g ml^{-1}$ hydrocortisone, and 1.2mM calcium at 100 % confluency and maintained for an additional 5–10 days (Uchida *et al*., 2001).

Silencing of VDR and coactivators

Keratinocytes (60mm dish for lipid analysis or 12 wells for RNA analysis) were infected with shRNA adenovirus (75 IFU per cell) (Hawker *et al*., 2007) for VDR, DRIP, SRC2, and SRC3 to block their expression in serum free CK media and maintained for 3 days for their proliferation. Cells were then switched to medium containing vitamin C and serum for 5–10 days to induce the formation of multilayered tissues.

VDR null mice

Animals heterozygous for the *Vdr* null mutation, *Vdr* tm1Ska, outbred to C57BL/6, were provided as a gift from Dr Shigeaki Kato (The University of Tokyo, Japan). Their development has been previously described (Yoshizawa *et al*., 1997). These mice were bred to provide the wild-type and homozygous mutant *Vdr* tm1Ska/*Vdr*tm1Ska littermates (hereafter referred to as VDR null mice) used for these studies. Genotyping was performed by PCR as described (Bikle *et al*., 2006). For these studies, the mice were raised on a 2% calcium, 1.25% phosphorus, 20% lactose diet (TD96348; Teklad, Madison, WI), which was previously shown to normalize mineral ion homeostasis and prevent rickets in these mice (Li *et al*., 1998). Under these conditions, the VDR null animals grew at approximately the same rate as their wild-type littermates. These studies were approved by the Animal Use Committee of the San Francisco VA Medical Center and were conducted in accordance with accepted standards of humane animal care, as outlined in the Ethical Guidelines.

Measurement of mRNA expression

Total RNA was isolated from keratinocytes using the RNeasy RNA purification kit (Qiagen, Valencia, CA), and cDNA was prepared using the reverse transcription kit (Applied Biosystems, Foster City, CA). mRNA expression of lipid synthesis enzymes was measured by quantitative real-time PCR using SYBR green (Applied Biosystems). Relative expression of these mRNAs compared to mitochondrial ribosomal protein L19 control mRNA was calculated. Primers for quantitative real-time PCR analysis were designed using Primer Express (Applied Biosystems) to span the exon and intron boundaries. Primer sequences will be provided on request. These experiments were repeated using at least three different batches of primary keratinocytes.

Lipid analysis

From cultured keratinocytes, total lipids were extracted from fully differentiated keratinocytes as described previously (Uchida *et al*., 2001). From VDR null mice, total lipids were extracted from epidermis, which was separated from dermis by incubation of the skin in phosphate-buffered saline at 60 °C for 45 seconds. The major lipid species were separated first by high-performance thin-layer chromatography (Uchida *et al*., 2001), with the following solvent systems: (1) for Cer and GlcCer: chloroform–methanol–water (40:10:1, v/v/v) to 2 cm and then to 5 cm; chloroform–methanol–acetic acid (47:2:0.5, v/v/v) to 8.5 cm; and *n*-hexane–diethyl ether–acetic acid (65:35:1, v/v/v) to the top of the plate; (2) for SM: chloroform–methanol–acetic acid–water (50:30:8:4, v/v); and (3) for cholesterol and FAs: *n*-hexane–diethyl ether–acetic acid (70:30:1, v/v/v) twice to top of the plate. Lipids were visualized after treatment with cupric acetate–phosphoric acid, and heating to 160 °C for 15 minutes. The

quantity of each lipid was determined by spectrodensitometry, as previously described (Holleran *et al*., 1997).

Electron microscopy

Human epidermal keratinocytes infected with the various adeno-viruses described above and maintained in the vitamin C and serum medium for 10 days were examined. Mouse skins were excised from 4- or 6-week-old wild-type or littermate VDR null mice. These samples were fixed in half-strength Karnovsky's fixative overnight, and postfixed with either 0.25% ruthenium tetroxide or 2% aqueous osmium tetroxide, both containing 1.5% potassium ferrocyanide, as previously described (Hou *et al*., 1991). For lanthanum tracer studies (Elias and Brown, 1978), skin biopsies were pretreated by floating them on a 4% lanthanum solution containing 4% sucrose, 0.05 M cacodylate, and 1% glutaraldehyde at pH 7.6 for 2 hours. Ultrathin sections were examined without further contrasting, or after treatment with lead citrate as a contrasting agent in an electron microscope (Zeiss 10A; Carl Zeiss, Thornwood, NY) operated at 60 kV. LB density and its content, lipid secretion and processing, and lanthanum incorporation were assessed visually in randomly photographed micrographs.

Ceramide glucosyltransferase activity

The UGCG activity was assessed by incorporation of glucose into GlcCer in keratinocytes as described previously (Chatterjee *et al*., 1975, 1996). Keratinocytes infected with shRNA adenovirus and maintained in the vitamin C system described earlier were metabolically labeled with [^{3}H]-galactose (1.5 μCi ml^{-1}) during the last 5 hours. Radiolabeled galactose taken into cells was converted to UDP-galactose, epimerized to UDP-glucose, and then utilized for GlcCer synthesis. Galactose was used as a substrate because it is more efficiently incorporated into GlcCer than glucose. Lipids were extracted and the GlcCer fraction was separated by high-performance thin-layer chromatography as mentioned in lipid analysis. Radioactivity in the GlcCer fraction was determined using a Beckman LS-1800 scintillation counter. UGCG activities (incorporated ^{3}H) were normalized to protein content (c.p.m. per mg protein).

Acknowledgments

We are grateful to Dr. Walter M. Holleran for discussions. We also thank Ms Sally Pennypacker for keratinocyte culture support, Nathaniel P. Hawker for adenovirus production and infection, and Arnaud Teichert for VDR null mice. This work was supported by NIH grants R01 AR050023 (DDB) and P01 AR39448 (DDB), AR051077 (YU), AR19098 (PME), AR39948 (PME) the Veterans Affairs Merit Review Program (DDB, PME), and the American Institute of Cancer Research (DDB).

Abbreviations

ABCA12	ATP-binding cassette transporter protein 12
Cer	ceramide
DRIP	vitamin D receptor-interacting protein
ELOVL	elongation of very long fatty acid
FA	fatty acid
FA2H	fatty acid 2-hydroxylase
GBA	β-glucocerebrosidase
GlcCer	glucosylceramide
LB	lamellar body

SC	stratum corneum
SG	stratum granulosum
shRNA	short-hairpin RNA
siRNA	short-interferance RNA
SM	sphingomyelin
SPT	serine palmitoyl transferease
SRC	steroid receptor coactivator
UGCG	ceramide glucosyltransferase
VDR	Vitamin D receptor

REFERENCES

Akiyama M, Sugiyama-Nakagiri Y, Sakai K, McMillan JR, Goto M, Arita K, et al. Mutations in lipid transporter ABCA12 in harlequin ichthyosis and functional recovery by corrective gene transfer. J Clin Invest 2005;115:1777–84. [PubMed: 16007253]

Bikle DD. Vitamin D regulated keratinocyte differentiation. J Cell Biochem 2004;92:436–44. [PubMed: 15156556]

Bikle DD, Elalieh H, Chang S, Xie Z, Sundberg JP. Development and progression of alopecia in the vitamin D receptor null mouse. J Cell Physiol 2006;207:340–53. [PubMed: 16419036]

Blazek E, Mittler G, Meisterernst M. The mediator of RNA polymerase II. Chromosoma 2005;113:399–408. [PubMed: 15690163]

Bourbon HM, Aguilera A, Ansari AZ, Asturias FJ, Berk AJ, Bjorklund S, et al. A unified nomenclature for protein subunits of mediator complexes linking transcriptional regulators to RNA polymerase II. Mol Cell 2004;14:553–7. [PubMed: 15175151]

Chatterjee S, Cleveland T, Shi WY, Inokuchi J, Radin NS. Studies of the action of ceramide-like substances (D- and L-PDMP) on sphingolipid glycosyltransferases and purified lactosylceramide synthase. Glycoconj J 1996;13:481–6. [PubMed: 8781979]

Chatterjee S, Sweeley CC, Velicer LF. Glycosphingolipids of human KB cells grown in monolayer, suspension, and synchronized cultures. J Biol Chem 1975;250:61–6. [PubMed: 1141212]

Elias PM. Stratum corneum defensive functions: an integrated view. J Invest Dermatol 2005;125:183–200. [PubMed: 16098026]

Elias PM. The skin barrier as an innate immune element. Semin Immunopathol 2007;29:3–14. [PubMed: 17621950]

Elias PM, Brown BE. The mammalian cutaneous permeability barrier: defective barrier function is essential fatty acid deficiency correlates with abnormal intercellular lipid deposition. Lab Invest 1978;39:574–83. [PubMed: 739761]

Elias PM, Menon GK. Structural and lipid biochemical correlates of the epidermal permeability barrier. Adv Lipid Res 1991;24:1–26. [PubMed: 1763710]

Gibson DF, Ratnam AV, Bikle DD. Evidence for separate control mechanisms at the message, protein, and enzyme activation levels for transglutaminase during calcium-induced differentiation of normal and transformed human keratinocytes. J Invest Dermatol 1996;106:154–61. [PubMed: 8592067]

Hamanaka S, Hara M, Nishio H, Otsuka F, Suzuki A, Uchida Y. Human epidermal glucosylceramides are major precursors of stratum corneum ceramides. J Invest Dermatol 2002;119:416–23. [PubMed: 12190865]

Hamanaka S, Takemoto T, Hamanaka Y, Asagami C, Suzuki M, Suzuki A, et al. Structure determination of glycosphingolipids of cultured human keratinocytes. Biochim Biophys Acta 1993;1167:1–8. [PubMed: 8461327]

Haussler MR, Whitfield GK, Haussler CA, Hsieh JC, Thompson PD, Selznick SH, et al. The nuclear vitamin D receptor: biological and molecular regulatory properties revealed. J Bone Miner Res 1998;13:325–49. [PubMed: 9525333]

Hawker NP, Pennypacker SD, Chang SM, Bikle DD. Regulation of human epidermal keratinocyte differentiation by the vitamin D receptor and its coactivators DRIP205, SRC2, and SRC3. J Invest Dermatol 2007;127:874–80. [PubMed: 17082781]

Holleran WM, Ginns EI, Menon GK, Grundmann JU, Fartasch M, McKinney CE, et al. Consequences of beta-glucocerebrosidase deficiency in epidermis. Ultrastructure and permeability barrier alterations in Gaucher disease. J Clin Invest 1994;93:1756–64. [PubMed: 8163674]

Holleran WM, Takagi Y, Uchida Y. Epidermal sphingolipids: metabolism, function, and roles in skin disorders. FEBS Lett 2006;580:5456–66. [PubMed: 16962101]

Holleran WM, Uchida Y, Halkier-Sorensen L, Haratake A, Hara M, Epstein JH, et al. Structural and biochemical basis for the UVB-induced alterations in epidermal barrier function. Photodermatol Photoimmunol Photomed 1997;13:117–28. [PubMed: 9453079]

Hou SY, Mitra AK, White SH, Menon GK, Ghadially R, Elias PM. Membrane structures in normal and essential fatty acid-deficient stratum corneum: characterization by ruthenium tetroxide staining and X-ray diffraction. J Invest Dermatol 1991;96:215–23. [PubMed: 1991982]

Jakobsson A, Westerberg R, Jacobsson A. Fatty acid elongases in mammals: their regulation and roles in metabolism. Prog Lipid Res 2006;45:237–49. [PubMed: 16564093]

Jennemann R, Sandhoff R, Langbein L, Kaden S, Rothermel U, Gallala H, et al. Integrity and barrier function of the epidermis critically depend on glucosylceramide synthesis. J Biol Chem 2007;282:3083–94. [PubMed: 17145749]

Jensen JM, Folster-Holst R, Baranowsky A, Schunck M, Winoto-Morbach S, Neumann C, et al. Impaired sphingomyelinase activity and epidermal differentiation in atopic dermatitis. J Invest Dermatol 2004;122:1423–31. [PubMed: 15175033]

Jensen JM, Forl M, Winoto-Morbach S, Seite S, Schunck M, Proksch E, et al. Acid and neutral sphingomyelinase, ceramide synthase, and acid ceramidase activities in cutaneous aging. Exp Dermatol 2005;14:609–18. [PubMed: 16026583]

Jensen JM, Schutze S, Forl M, Kronke M, Proksch E. Roles for tumor necrosis factor receptor p55 and sphingomyelinase in repairing the cutaneous permeability barrier. J Clin Invest 1999;104:1761–70. [PubMed: 10606630]

Kornberg RD. Mediator and the mechanism of transcriptional activation. Trends Biochem Sci 2005;30:235–9. [PubMed: 15896740]

Leo C, Chen JD. The SRC family of nuclear receptor coactivators. Gene 2000;245:1–11. [PubMed: 10713439]

Li JJ, Kim RH, Zhang Q, Ogata Y, Sodek J. Characteristics of vitamin D3 receptor (VDR) binding to the vitamin D response element (VDRE) in rat bone sialoprotein gene promoter. Eur J Oral Sci 1998;106 (Suppl 1):408–17. [PubMed: 9541257]

Motta S, Monti M, Sesana S, Caputo R, Carelli S, Ghidoni R. Ceramide composition of the psoriatic scale. Biochim Biophys Acta 1993;1182:147–51. [PubMed: 8357845]

Ng DC, Shafaee S, Lee D, Bikle DD. Requirement of an AP-1 site in the calcium response region of the involucrin promoter. J Biol Chem 2000;275:24080–8. [PubMed: 10816578]

Oda Y, Ishikawa MH, Hawker NP, Yun QC, Bikle DD. Differential role of two VDR coactivators, DRIP205 and SRC-3, in keratinocyte proliferation and differentiation. J Steroid Biochem Mol Biol 2007;103:776–80. [PubMed: 17223341]

Oda Y, Sihlbom C, Chalkley RJ, Huang L, Rachez C, Chang CP, et al. Two distinct coactivators, DRIP/mediator and SRC/p160, are differentially involved in vitamin D receptor transactivation during keratinocyte differentiation. Mol Endocrinol 2003;17:2329–39. [PubMed: 12893881]

Robson KJ, Stewart ME, Michelsen S, Lazo ND, Downing DT. 6-Hydroxy-4-sphingenine in human epidermal ceramides. J Lipid Res 1994;35:2060–8. [PubMed: 7868984]

Schauber J, Oda Y, Buchau AS, Yun QC, Steinmeyer A, Zugel U, et al. Histone acetylation in keratinocytes enables control of the expression of cathelicidin and CD14 by 1,25-dihydroxyvitamin D(3). J Invest Dermatol 2008;128:816–24. [PubMed: 17943182]

Schurer NY, Elias PM. The biochemistry and function of stratum corneum lipids. Adv Lipid Res 1991;24:27–56. [PubMed: 1763715]

Sidransky E, Fartasch M, Lee RE, Metlay LA, Abella S, Zimran A, et al. Epidermal abnormalities may distinguish type 2 from type 1 and type 3 of Gaucher disease. Pediatr Res 1996;39:134–41. [PubMed: 8825398]

Thomas AC, Cullup T, Norgett EE, Hill T, Barton S, Dale BA, et al. ABCA12 is the major harlequin ichthyosis gene. J Invest Dermatol 2006;126:2408–13. [PubMed: 16902423]

Uchida Y, Behne M, Quiec D, Elias PM, Holleran WM. Vitamin C stimulates sphingolipid production and markers of barrier formation in submerged human keratinocyte cultures. J Invest Dermatol 2001;117:1307–13. [PubMed: 11710949]

Uchida Y, Hama H, Alderson NL, Douangpanya S, Wang Y, Crumrine DA, et al. Fatty acid 2-hydroxylase, encoded by FA2H, accounts for differentiation-associated increase in 2-OH ceramides during keratinocyte differentiation. J Biol Chem 2007;282:13211–9. [PubMed: 17355976]

Uchida YH, Holleran WM. Omega-O-acylceramide, a lipid essential for mammalian survival. J Dermatol Sci 2008;51:77–87. [PubMed: 18329855]

Vasireddy V, Uchida Y, Salem N Jr, Kim SY, Mandal MN, Reddy GB, et al. Loss of functional ELOVL4 depletes very long-chain fatty acids (> or =C28) and the unique omega-*O*-acylceramides in skin leading to neonatal death. Hum Mol Genet 2007;16:471–82. [PubMed: 17208947]

Westerberg R, Tvrdik P, Unden AB, Mansson JE, Norlen L, Jakobsson A, et al. Role for ELOVL3 and fatty acid chain length in development of hair and skin function. J Biol Chem 2004;279:5621–9. [PubMed: 14581464]

Xie Z, Komuves L, Yu QC, Elalieh H, Ng DC, Leary C, et al. Lack of the vitamin D receptor is associated with reduced epidermal differentiation and hair follicle growth. J Invest Dermatol 2002;118:11–6. [PubMed: 11851870]

Yoshizawa T, Handa Y, Uematsu Y, Takeda S, Sekine K, Yoshihara Y, et al. Mice lacking the vitamin D receptor exhibit impaired bone formation, uterine hypoplasia and growth retardation after weaning. Nat Genet 1997;16:391–6. [PubMed: 9241280]

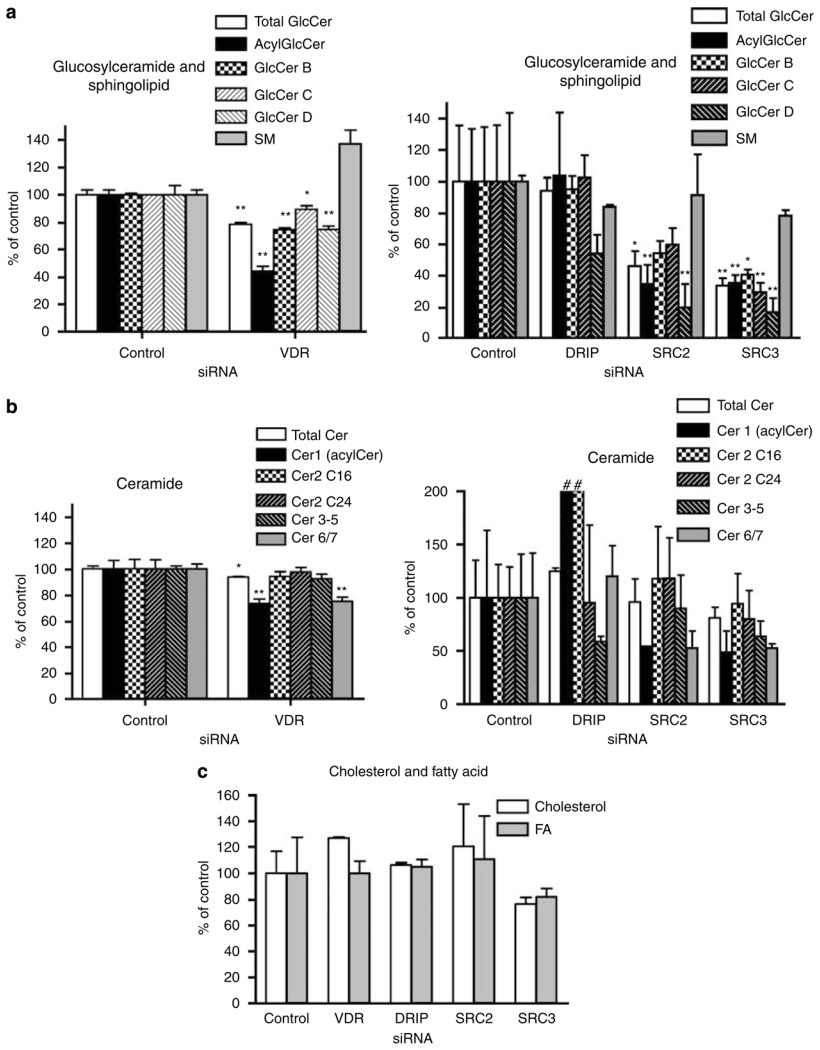

Figure 1. VDR and coactivators SRC2- and 3-regulated production of specific GlcCer species

Human epidermal keratinocytes were infected with shRNA adenovirus for VDR to block its expression and compared to keratinocytes infected by control adenovirus (**a** and **b**, left graphs). The expression of DRIP, SRC2, and SRC3 was also blocked by adenovirus infection and compared to control (**a** and **b**, right graphs). Keratinocytes were maintained in medium supplemented with vitamin C and serum to induce lipid production (Uchida *et al*., 2001). The immediate precursors of Cer, GlcCer, and SM (**a**); Cer (**b**); cholesterol (**c**); and FA (**c**); were analyzed. The lipid contents were normalized to protein content (μg per mg protein). Relative contents compared to keratinocytes infected by control adenovirus were calculated and expressed as percent of control. GlcCer was further separated into four fractions by HPTLC (**a**, acylGlcCer, GlcCer B, C, and D). Cer was separated into five species (**b**, Cer 1(acylCer), Cer 2 (amide-linked C16 or C24 FA), Cer 3–5, Cer 6/7). The characterization of GlcCer species and deduced Cer are shown in Table 1. Data are represented as mean and standard deviation (SD) of three measurements. All data were analyzed by Student's *t*-test and statistical significance compared to control group is shown with asterisks (*P<0.01, **P<0.03). Increases over 200% are shown by #.

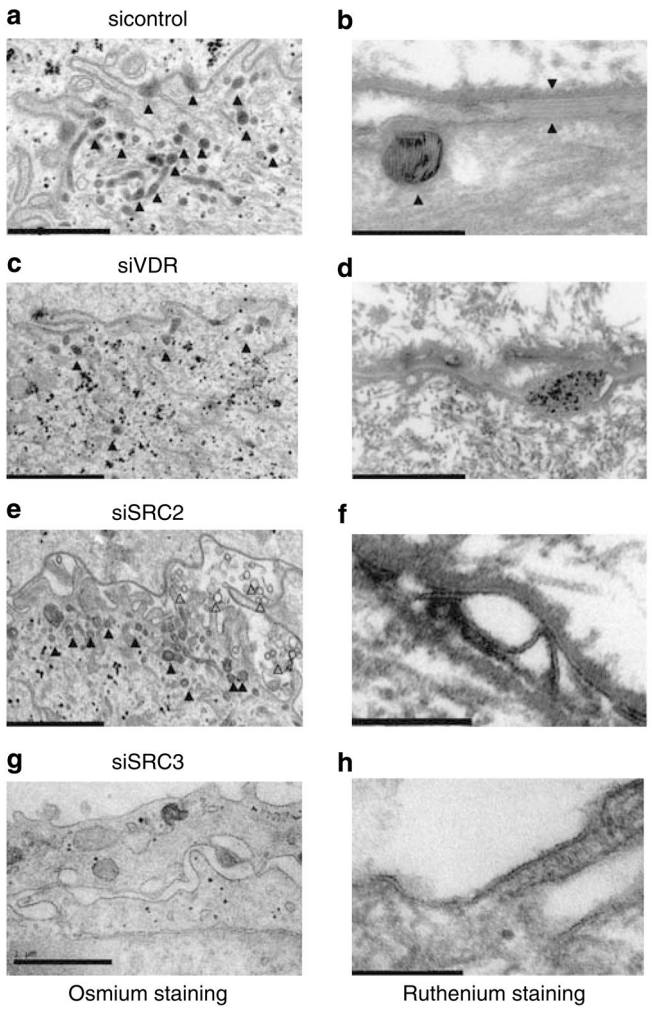

Figure 2. VDR and coactivators SRC2 and 3 are critical for barrier marker formation

Expression of VDR (**c**, **d**), SRC2 (**e**, **f**), SRC3 (**g**, **h**) was blocked and compared to control (**a**, **b**). The tissues were observed under electron microscopy to determine number of LBs and their content (**a**, **c**, **e**, and **g**). The presence of LB is shown by triangles. The lipid secretion and processing was evaluated using ruthenium staining (**b**, **d**, **f**, and **h**). Control tissues showed a substantial number of LB with replete internal lamellar content (**b**, left triangle). Normal lipid secretion and processing were shown by lipid bilayers between two right triangles (**b**). When VDR was silenced, fewer LB (**c**, shown by triangles) with lack of lamellar structure (**d**) were observed. Lipid secretion and processing were incomplete (**d**) compared to control (**b**). SRC2 silencing also resulted in abnormal LB formation (**e**, triangles) lacking proper lamellar structure (**e**, **f**) and abnormal lipid processing (**f**). Unusual empty vesicles were also observed in the extracellular space (**e**, open triangles). SRC3 silencing abolished the whole process as shown by no LB and no lipid bilayers (**g**, **h**). Bars represent 1.0 μm (**a**, **c**, **e**, and **g**) and 0.2 μm (**b**, **d**, **f**, and **h**).

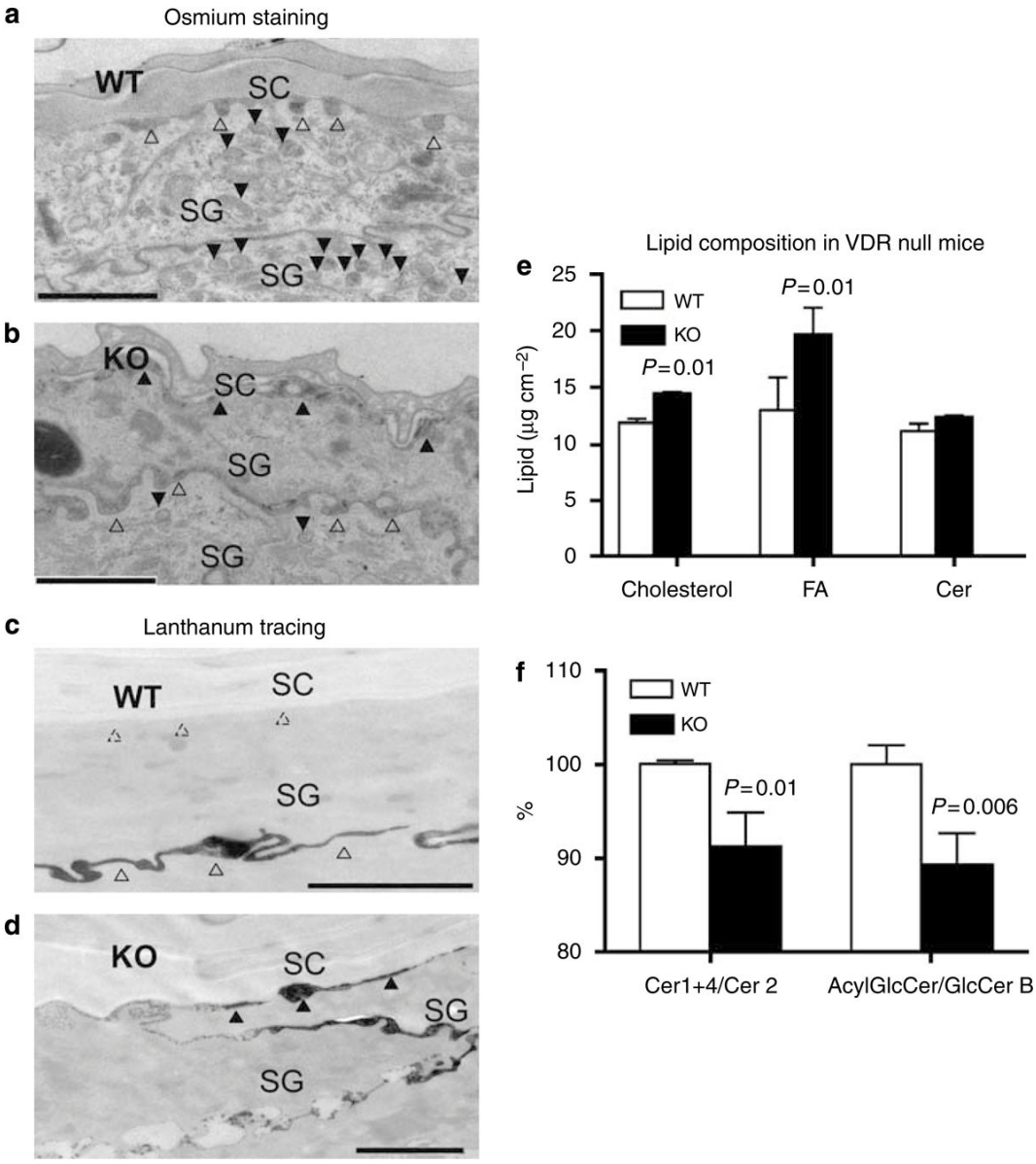

Figure 3. Targeted disruption of VDR resulted in abnormalities in LB formation, lipid secretion and functional barrier formation, and altered lipid composition in mouse skin

Skin biopsies from 6-week-old wild-type (WT) (a, c) and VDR knockout (KO) mice (b, d) were fixed and stained with osmium tetroxide. Sections were visualized by electron microscopy. A substantial number of LB was observed (a, closed triangles) with secretion of LB contents at the SG–SC interface in WT mice (a, open triangles). In contrast, VDR null mice showed decreased numbers of LBs with decreased content (b, closed triangles in lower SG). Abnormal lipid secretion was shown by disorganized structures at the SG–SC interface (b, closed triangles in lower SG) as well as at SG–SG junctions (b, open triangles). To assess whether defective permeability barrier homeostasis can be attributed to the abnormalities in LB formation and secretion, we assessed the functional barrier by lanthanum perfusion, which serves as an electron-dense tracer of water movement through the epidermis. In WT skin, tracer was restored to extracellular spaces of the nucleated cell layers (c, open triangles), but completely excluded from the SG–SC interface (c, dashed triangles). In contrast, VDR null

mice showed abundant tracer traversing the SG–SC space (d, closed triangles), indicating that the lipid processing and secretion abnormalities are associated with, and likely the cause of the defective barrier to the extracellular movement of water. Bars represent 1 μm (a–d). Total lipids were extracted from the epidermis of bothWT and VDR null mice (7 weeks old). Three major barrier lipids, cholesterol, FA, and Cer, were analyzed and expressed as μg cm^{-2} epidermis (e). Cer was further separated into six fractions (Table 3). To assess the proportion of epidermis-unique species (acylCer, Cer 4) to the major constituent of Cer (Cer 2), the ratio was calculated (Cer 1+4/Cer2) (f). GlcCer was also separated into 4 fractions (Table 3), and ratio of epidermis-unique species of acylGlcCer to GlcCer B (major species in undifferentiated keratinocytes) was calculated (f). The characterization of GlcCer species and deduced Cer are shown in Table 1. Data are represented as the mean and standard deviation (SD) of three measurements. All data were analyzed by Student's t-test, and the statistical significance of the differences between VDR null mice and WT is shown as P-values.

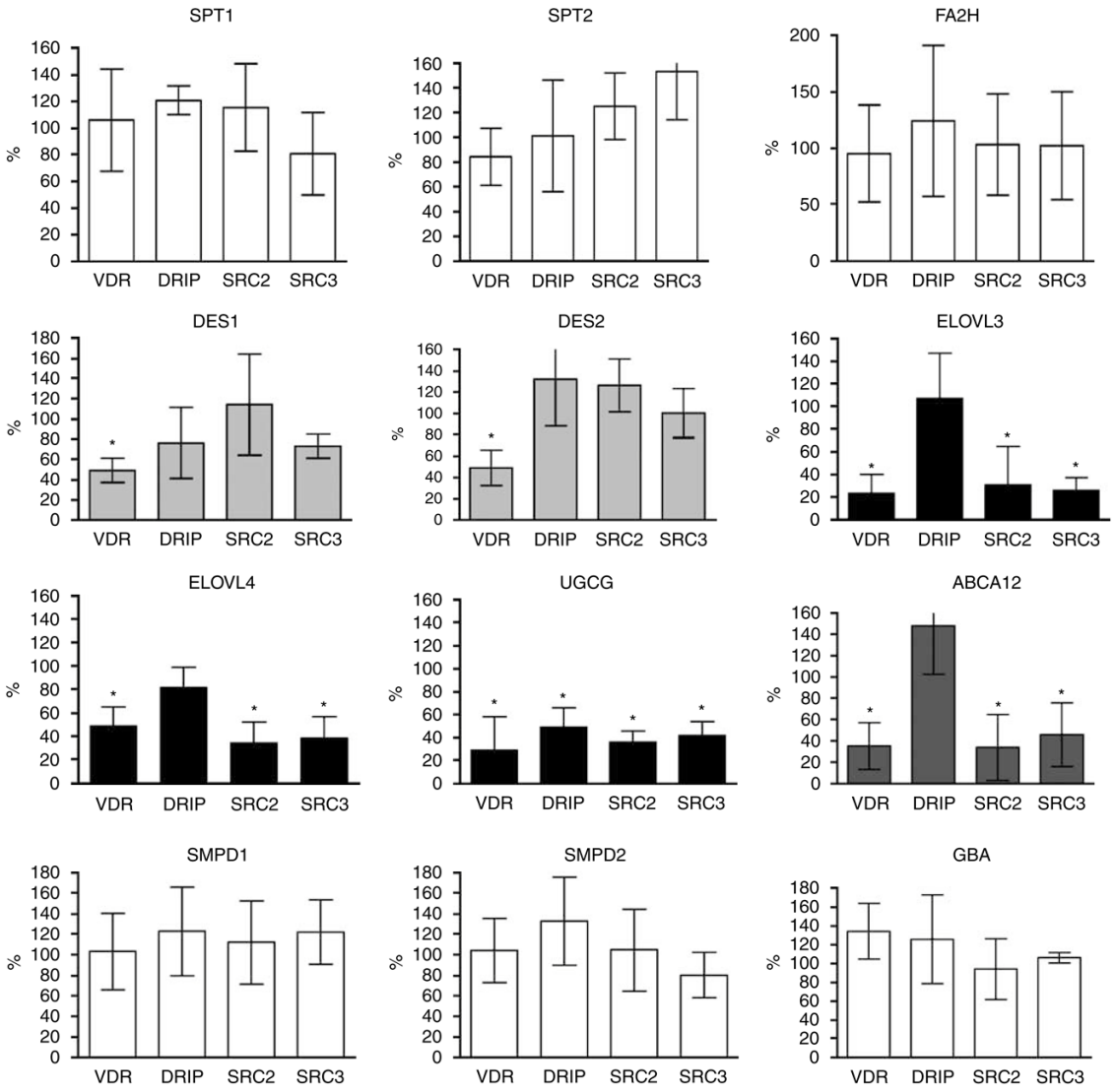

Figure 4. VDR, SRC2, and SRC3 regulate mRNA expression of GlcCer synthesis enzymes and the lipid transporter ABCA12

Human epidermal keratinocytes were infected with shRNA adenovirus for VDR, DRIP, SRC2, and SRC3 to block their expression. Cells were maintained with vitamin C and serum medium to induce barrier formation. The transcription of lipid synthesis enzymes was evaluated by quantitative real-time PCR. The mRNA levels were normalized to control gene L19, and relative expression to control group was expressed as a percentage (%). Data are represented as mean and standard deviation (SD) of at least three independent experiments. All data were analyzed by t-test, and statistical significance compared to control group is shown with asterisks (*$P<0.01$).

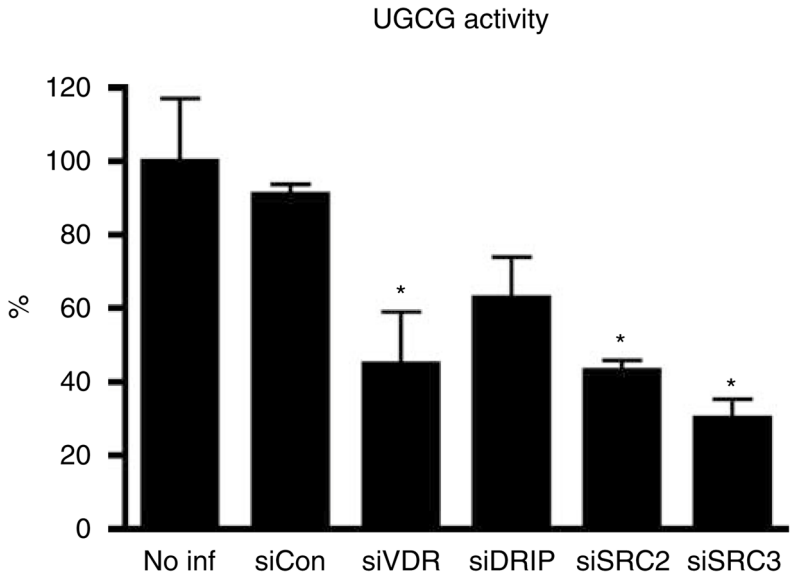

Figure 5. VDR, SRC2, and SRC3 regulate the enzyme activity of UGCG

The expression of VDR and coactivators was blocked as described in Figure 4. The enzyme activity of UGCG was measured by metabolic labeling of GlcCer. The incorporated radioactivity was normalized to protein amounts (c.p.m. per mg protein), and relative activity compared to noninfected keratinocytes was expressed as a percentage (%). Data are represented as the mean and standard deviation (SD). All data were analyzed by *t*-test, and the statistical significance of the differences between experimental and a control group is shown with asterisks (*P<0.01).

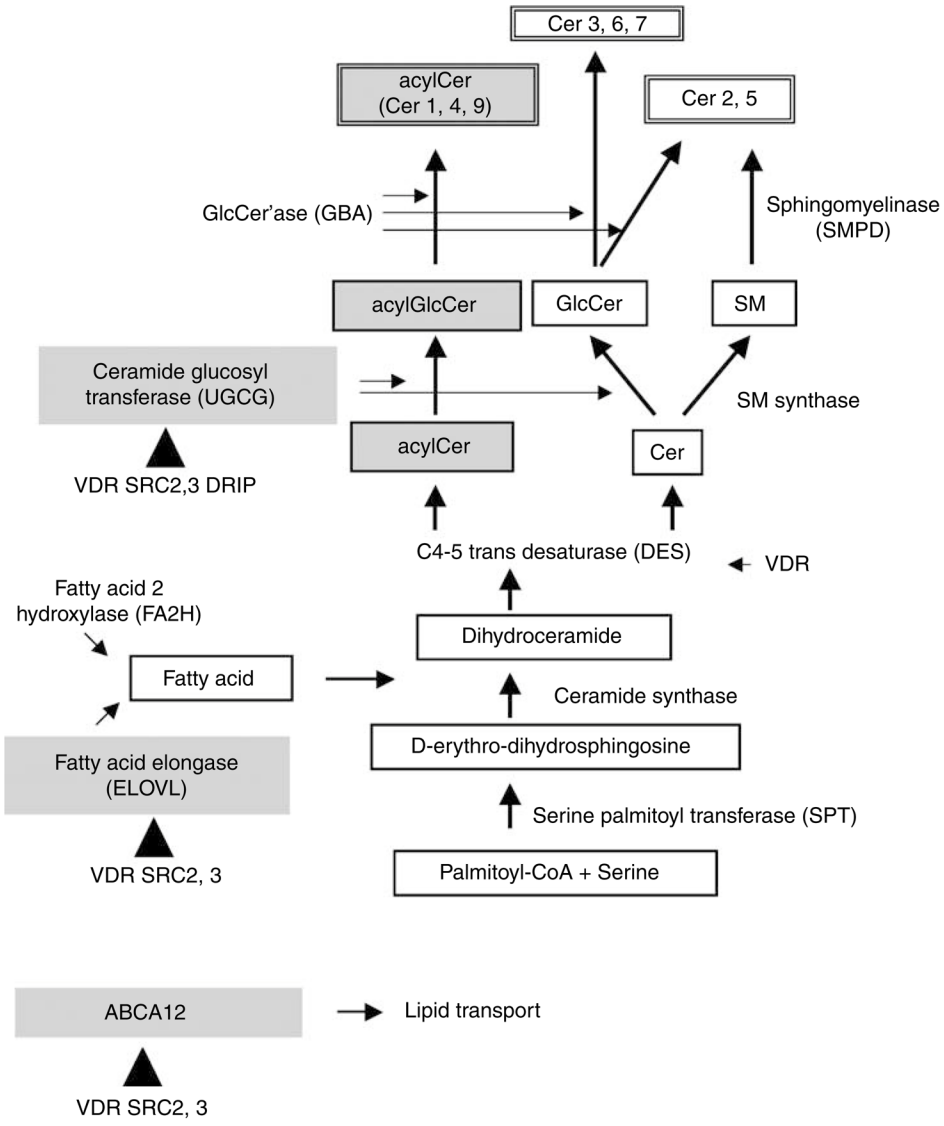

Figure 6. VDR and coactivators SRC2 and 3 regulate ELOVL and UGCG involved in synthesis of acylCer/acylGlcCer in epidermis

The lipid transporter ABCA12 also was regulated by VDR and coactivators. The synthetic pathways for the Cer/GlcGlc and enzymes required for each process are shown. The enzymes ELOVL, UGCG, and ABCA12 are highlighted, and their regulation by VDR, SRC2, and 3 is shown by triangles.

Table 1

Four different GlcCer species deduced to the different ceramides

	Ceramide moieties[1]		
	Amide-linked FA[2]	**Sphingol**[3]	**SC Cer**[4]
AcylGlcCer	C30-34ωh	S	Cer 1(EOS), Cer 4(EOH)
GlcCer B	C16-24	S, P	Cer 2 (NS), Cer 3 (NP)
GlcCer C	C16-26, C26αh	S, P	Cer 3 (NP), Cer 5 (AS)
GlcCer D	C18-26, C24-26αh	S, P, D	Cer 5 (AS), Cer 6 (AP), Cer7(AH)

[1] Ceramide moieties were previously described (Hamanaka *et al*., 1993; Hamanaka *et al*., 2002).

[2] Carbon chain lengths of amide-linked FA; ωh, omega-hydroxy; αh, α(2)hydroxy.

[3] S, sphingosine; P, phytosphingosine (or 4-hydroxysphinganine); H, 6-hydroxysphingosine.

[4] Deduced Cer species in the stratum corneum species generated from GlcCer. Abbreviations for Cer structures are according to (Motta *et al*., 1993; Robson *et al*., 1994). N, A, and EO indicate amide-linked FA species: N, non-OH FA; A, α-OH FA; EO, ω–*O*-esterified FA. A, S, P, and H indicate sphingol structures. Cer 2 (NS) are ubiquitously expressed in mammalian tissues, whereas late stages of differentiation produce heterogenous Cer species. In particular, Cer 1 (EOS), Cer 4 (EOH), and Cer 9 (EOP) are unique to the epidermis. GlcCer were separated into four different species, acylGlcCer, GlcCer B, C, and D. They contain different amide linked FA and sphingols. Each species is deduced to 9 different Cer (Cer 1–9).

Table 2

Silencing of VDR, SRC2, and SRC3, but not DRIP, resulted in abnormal barrier marker formation

siRNA	Stratification	LB numbers	LB contents	Lipid secretion/processing
Control	Complete	+++	Normal	Normal
VDR	Incomplete	+	Abnormal	Abnormal
DRIP	Incomplete	+++	Normal	Normal
SRC2	No	+++	Abnormal	Abnormal
SRC3	No	No LB	Not evident	Not evident

The expression of VDR and coactivators DRIP, SRC2, SRC3 were blocked in human epidermal keratinocytes using siRNA-silencing technology. Cells were maintained in a submerged culture system supplemented with vitamin C and serum for 10 days to allow barrier formation. The morphology of cultured tissues was analyzed using electron microscopy. Their ability to carry out three key steps in epidermal barrier formation; stratification, LB formation/content, and lipid secretion/processing; was examined and is summarized in this table.

Table 3

Cer/GlcCer content in VDR null mice (μg per cm^2 epidermis)

	Total Cer	Cer 1(acylCer)	Cer 2	Cer 3	Cer 4	Cer 5	Cer6/7
WT	11.1±0.63	1.69±0.05	5.43±0.16	2.07±0.10	0.57±0.09	1.07±0.17	0.42±0.03
KO	12.3±0.18	1.71±0.05	6.01±0.09	2.38±0.06	0.58±0.03	0.91±0.06	0.66±0.04
P-values	NS	NS	0.01	0.01	NS	NS	0.01

	Total GlcCer	acylGlcCer	GlcCer B	GlcCer C	GlcCer D
WT	2.61±0.05	1.19±0.01	0.76±0.02	0.36±0.01	0.30±0.03
KO	2.87±0.13	1.15±0.03	0.83±0.04	0.46±0.03	0.44±0.04
P-values	NS	NS	NS	0.01	0.01

Total lipids were extracted from epidermis of wild-type (WT) and VDR null (KO) mice (7 weeks old). The cholesterol, FA, Cer, GlcCer, SM were analyzed. Cer was further separated into 6 fractions by HPTLC (Cer 1:acylCer, Cer 2, Cer 3. Cer 4, Cer 5, Cer 6–7). Cer 2 is the major species and constitutively produced. Cer 1 (acylCer) and Cer 4 are generated from acylGlcCer, which is epidermis-unique species and increase at a late stage of differentiation. GlcCer was also further separated into 4 fractions (acylGlcCer, GlcCer B, C, and D). The acylGlcCer is epidermis-specific species. GlcCer B generates Cer 2, the major constituent of Cer. The proportions of epidermis unique species vs general constituents (Cer 1±4/Cer, acylGlcCer/GlcCer B) were calculated and shown in Figure 3f. SM decreased by 15%. Data are represented as mean and standard deviation (SD) of three measurements. All data were analyzed by Student's *t*-test and statistical significance of VDR null mice compared to wild type is shown with *P*-values. NS means not significant.